Journal of Photochemistry and Photobiology A: Chemistry 153 (2002) 83–88

Journal of Photochemistry and Photobiology A:Chemistry

www.elsevier.com/locate/jphotochem

Photophysical properties of novel [1,2,3]triazolo[4,5-d] pyridazine derivatives

Krisztina Nagy, László Biczók*, Attila Demeter, Péter Kövér, Zsuzsanna Riedl

Chemical Research Center, Hungarian Academy of Sciences, P.O. Box 17, 1525 Budapest, Hungary

Received 9 April 2002; received in revised form 25 June 2002; accepted 16 July 2002

Abstract

Photostability, fluorescence properties and triplet yield of [1,2,3]triazolo[4,5-d]pyridazine derivatives have been studied in various solvents. The energy of the lowest singlet excited state significantly decreases in the series of **1**, **2**, and **3**, and the latter compound emits negligible fluorescence. All substances are photochemically very stable. No photodecomposition occurs from singlet excited state and the triplet molecules do not react with alcohol showing that the lowest triplet state has $\pi\pi^*$ character. Internal conversion is found to be the dominant singlet excited state depopulating process. The short fluorescence lifetime of **2** is attributed to the particularly rapid non-radiative transition to the ground state. Both **1** and **2** readily form hydrogen-bonded complex with hexafluoroisopropanol. Light absorption does not enhance the hydrogen bonding power, therefore; no fluorescence quenching but fluorescence yield enhancement is observed.

Keywords: Fluorescence; Intersystem crossing; Internal conversion; Hydrogen bonding

1. Introduction

Substituted derivatives of 3(2H)-pyridazinone have received a widespread interest because a lot of them exhibit pharmaceutical, herbicidal or pesticidal activity [1]. Despite the large number of patents and papers dealing with the synthesis and application of these substances, their photophysical properties have not been studied. [1,2,3]Triazolo[4,5-d]pyridazines are precursors for the synthesis of new insensitive, energetic materials [2]. Photolysis of 1-aryl-1H-1,2,3-triazoles can be employed to prepare indol derivatives via photocyclization accompanied by denitrogenation [3].

A unique valence bond isomerization has recently been found which provides a simple synthetic pathway to the triazolopyridazinone derivatives [4]. As extension of this study, the main goal of the present paper is to reveal the photostability and the photophysical properties of these compounds and determine the major factors governing the rate of their various excited state deactivation processes. Special attention is devoted to the effect of hydrogen bonding. The formulas of the investigated substances are presented in Fig. 1.

2. Experimental details

5-Methyl-7-phenyl-2,5-dihydro-[1,2,3]triazolo[4,5-d]pyridazin-4-one (**1**), (5-methyl-7-phenyl-2,5-dihydro-[1,2,3]-triazolo[4,5-d]pyridazin-4-ylidene)-pyridin-2-yl-amine (**2**) and [2-(4-chloro-phenyl)-5-methyl-7-phenyl-2,5-dihydro-[1,2,3]triazolo[4,5-d]pyridazin-4-ylidene]-pyridin-2-yl-amine (**3**) were synthesised as described previously [4]. Solvents (Aldrich, HPLC grade), perylene (Aldrich) and 1,1,1,3,3,3-hexafluoro-2-propanol (Aldrich) were used as received. The UV-Vis absorption spectra were obtained with a Hewlett-Packard 8452 diode-array spectrophotometer. Corrected fluorescence spectra were recorded on a home-built spectrofluorimeter equipped with a Princeton Applied Research type 1140 A/B photon-counting system. Fluorescence quantum yields were determined relative to that of quinine sulfate in a 1N H_2SO_4 solution, for which a reference yield of 0.546 was used [5]. Fluorescence lifetimes were measured with time-correlated single-photon counting technique. If the samples did not absorb at 400 nm, an Applied Photophysics SP-3 apparatus with a hydrogen lamp was used. Otherwise, 400 nm light of a Picoquant diode laser (pulse duration 60 ps FWHM) excited the solution and the fluorescence decay was detected with a Hamamatsu H5783 photosensor module which was connected to a Picoquant Timeharp 100 electronics. Data were analysed by a non-linear least-squares deconvolution method. The

---

* Corresponding author. Tel.: +36-1-438-4143x564; fax: +36-1-325-7554.
E-mail address: biczok@chemres.hu (L. Biczók).

1010-6030/02/$ – see front matter © 2002 Published by Elsevier Science B.V.
PII: S1010-6030(02)00301-5

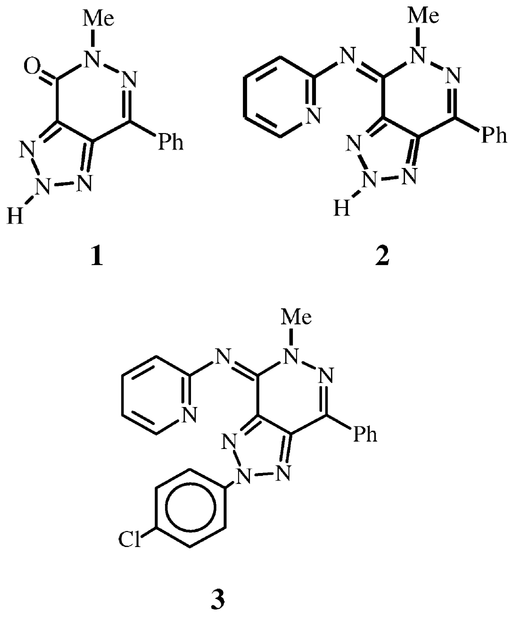

Fig. 1. Formulas of the investigated compounds.

fluorescence decays could be well described with a single exponential function. Triplet–triplet absorption was studied with the XeCl excimer laser flash photolysis apparatus described in our previous paper [6].

3. Results and discussion

3.1. Absorption and fluorescence spectra

Fig. 2 presents the absorption and the fluorescence spectra in toluene and ethanol, whereas the maxima of the bands are given in Table 1. The first absorption band of all three compounds exhibits hypsochromic shift going from toluene to ethanol. Vibration structure in the first band appears only for **2**, where not only the location of the maximum but also the shape of the absorption spectrum is solvent dependent. Introduction of the 4-chloro-phenyl moiety into the triazine ring of compound **2** results in loss of the vibration structure in the lowest energy band and absorbance enhancement in the second band (Fig. 2b). The fluorescence spectra for **1** are mirror symmetrical with the long-wavelength band of the absorption spectra but the large Stokes shift as well as the opposite displacement in the fluorescence and absorption spectra with increasing solvent polarity indicates significant change in the molecular structures upon excitation. The considerable Stokes shift is typical of carbonyl compounds; alkanones and cycloalkanones exhibit analogous behaviour. The spectra for **2** show blue-shift and much smaller gap appears between the fluorescence and absorption maxima. Compound **3** is so weakly fluorescent that negligible emission was observed in its solutions. Therefore, detailed studies were carried out only with **1** and **2**. The S_1 energies obtained from the location of the intersection of the normalised absorption and fluorescence spectra are given in the fourth column of Table 1. It is seen that for **2** the lowest excited singlet state energy ($E(S_1)$) rises with increasing $E_T(30)$ solvent polarity parameter. However, in the case of **1**, the change in $E(S_1)$ seems to correlate with the dielectric constant of the media.

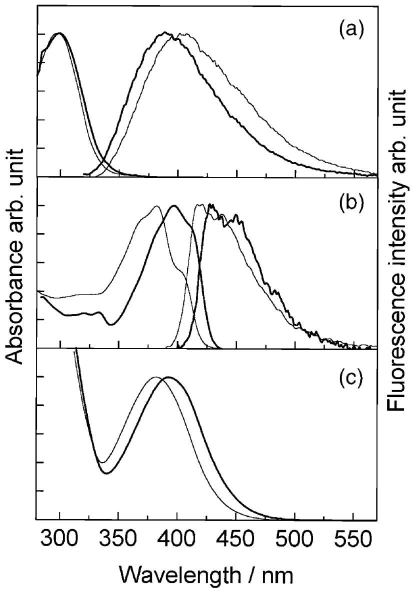

Fig. 2. Absorption and fluorescence spectra of: (a) **1**; (b) **2**; and (c) **3** in toluene (heavy line) and ethanol (thin line).

3.2. Effect of hydrogen bonding

In order to reveal whether hydrogen bonding interaction influences the photophysical properties, we used 1,1,1,3,3,3-hexafluoro-2-propanol (HFIPA) additive, which has high hydrogen bond donating power. The low acidity of HFIPA ($pK_a = 9.3$ in water [7]) ensures that it is not able to protonate **1**, **2** and **3**. Studies were carried out in toluene because the strongest hydrogen bonding is expected in apolar media. Addition of HFIPA leads to characteristic change in the absorption spectra as it is shown in Fig. 3. Slight alteration appears for **1**, whereas hypsochromic shift and change in the relative intensity of the vibrational structure of the absorption band are observed for **2**. The clear isosbestic point at 382 nm in the latter case demonstrates that 1:1 hydrogen-bonded complex formed. The inserts in Fig. 3 present the variation of the absorbance in the function of the HFIPA concentration. The equilibrium constant of hydrogen-bonding (K) can be determined using the following relationship:

$$A_\lambda = \frac{A^0_\lambda(1 + (\varepsilon_C/\varepsilon_F)_\lambda K[\text{HFIPA}])}{(1 + K[\text{HFIPA}])} \tag{1}$$

where $(\varepsilon_C/\varepsilon_F)_\lambda$ is the ratio of the molar absorption coefficients for the complexed and free compound at a particular wavelength (λ), A^0_λ and A_λ denote the absorbances in the presence and the absence of HFIPA, respectively. Non-linear

Table 1
Photophysical parameters of [1,2,3]-triazolo [4,5-d] pyridazine derivates and their hydrogen bond complexes with HFIPA in various solvents at 295 K

Solvent	ε[a]	$E_T(30)$[b] ($kJ\,mol^{-1}$)	$E(S_1)$ ($kJ\,mol^{-1}$)	λ_{abs} (nm)	λ_F (nm)	Φ_{ISC}	τ_F (ns)	Φ_F (10^{-2})	Φ_{IC}	k_{ISC} ($10^8\,s^{-1}$)	k_{IC} ($10^8\,s^{-1}$)	k_F ($10^7\,s^{-1}$)
1												
Toluene	2.38	142	354	299	388	0.23	1.2	3.1	0.74	1.9	6.2	2.6
Acetonitrile	37.5	193	349	299	405	0.34	2.0	4.2	0.62	1.7	3.1	2.1
Ethanol	24.55	217	353	296	405	0.21	1.9	3.3	0.76	1.1	4.0	1.7
1-HFIPA complex												
Toluene	2.38	142	352	300	405	0.35	2.0	3.9	0.61	1.8	3.1	2.0
2												
Toluene	2.38	142	286	410[c]	428	0.07	0.34	2.4	0.91	2.1	27	7.1
Acetonitrile	37.5	193	291	402	423	0.05	0.33	2.7	0.92	1.5	28	8.2
Ethanol	24.55	217	293	382	419	0.06	0.44	4.1	0.90	1.4	20	9.3
2-HFIPA complex												
Toluene	2.38	142	287	409	426	[d]	0.69	5.9	0.94	[d]	14	8.6

[a] Dielectric constant of the solvent [18].
[b] Solvent polarity parameter [18].
[c] Shoulder at low energy.
[d] Too small to measure.

least squares fit of this function to the absorbances gives the value of the two unknown parameters, K and $(\varepsilon_C/\varepsilon_F)_\lambda$. The line in the insert exhibits the best fit, which provides 57 ± 6 and $215 \pm 9\,M^{-1}$ for the hydrogen bonding equilibrium constant of **1** and **2**, respectively.

As it is seen in Fig. 4, addition of HFIPA to the solution of **1** leads to only slight fluorescence intensity enhancement and red-shift of the fluorescence maximum. However, in the case of **2**, the fluorescence becomes more intense. The inserts display the variation of fluorescence quantum yield in the function of the HFIPA concentration. It is well known that fluorescence yield is in general a complicated function of the hydrogen bonding additive concentration [8], however, several authors have demonstrated that an equation of the following type can reproduce usually quite well the variation

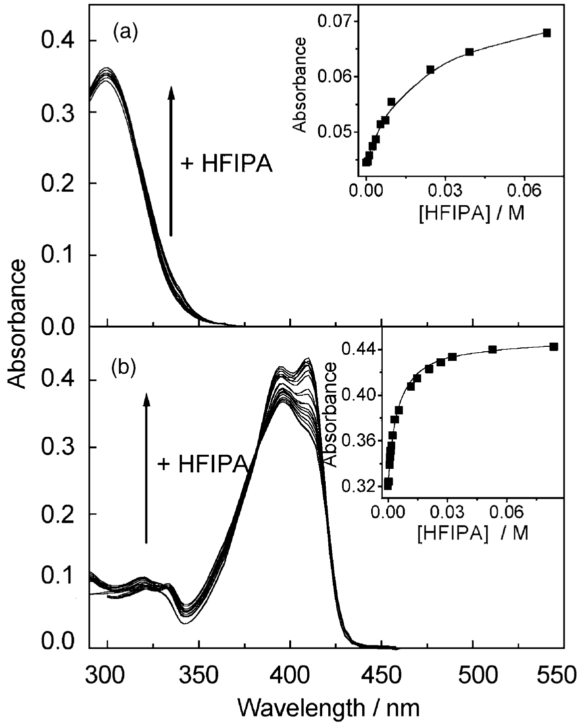

Fig. 3. Effect of hydrogen bonding on the absorption spectra of: (a) **1** and (b) **2** in toluene. Inserts display the absorbance change in the function of HFIPA concentration at 336 and 410 nm for **1** and **2**, respectively.

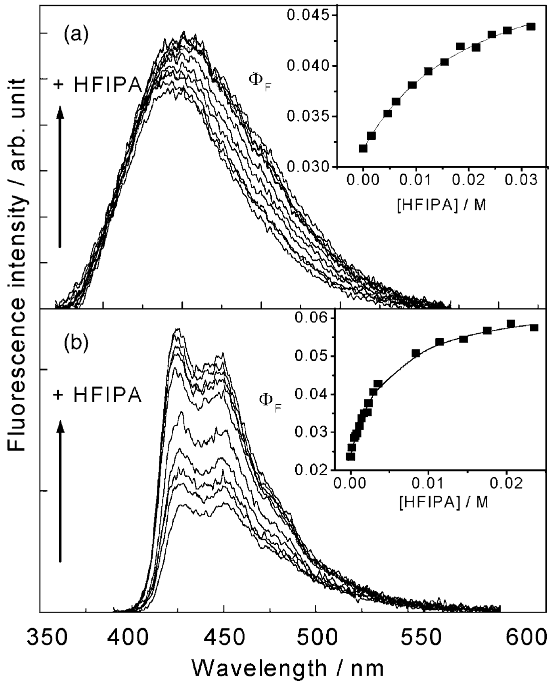

Fig. 4. Effect of hydrogen bonding on the fluorescence spectra of: (a) **1** and (b) **2** in toluene. Inserts give the change of the fluorescence yield in the function of HFIPA concentration.

of the fluorescence yield [8]:

$$\Phi_{\mathrm{F}} = \frac{\Phi_{\mathrm{F}}^{0}(1 + a[\mathrm{HFIPA}])}{(1 + b[\mathrm{HFIPA}])} \tag{2}$$

where Φ_{F} and Φ_{F}^{0} denotes the fluorescence yield in the presence and the absence of HFIPA, respectively, a and b are constants characteristic of the system. The inserts in Fig. 4 show that the experimental results can be described well with Eq. (2). The b parameters of the best fit are 47 ± 6 and $219 \pm 10\,\mathrm{M}^{-1}$ for **1** and **2**, respectively. The good agreement of these values with the equilibrium constants derived from absorption spectroscopic studies implies that the rate constants of hydrogen bond formation and decomposition are small compared with the decay constant of free and hydrogen-bonded excited molecules, respectively. In this case, b parameter represents the equilibrium constant of hydrogen bonding in the ground state.

3.3. *Quantum chemical calculations*

To reveal the electron distribution of the studied compounds in the ground and the excited states, quantum chemical calculations were carried out using semi-empirical and Hückel MO methods. The relative change in the energy of the lowest singlet excited state ($E(\mathrm{S}_1)$) in the series of the three studied compounds is described best by the Hückel MO method. Therefore, the results of these calculations are presented in Fig. 5. The AM-1 method gave slightly smaller difference between the $E(\mathrm{S}_1)$ of **1** and **2** than the experimentally found value but the conclusions based on the semi-empirical and the Hückel MO calculations agreed well. In the ground state the largest negative charge density is located on the oxygen of the carbonyl group and the nitrogen of the Schiff base moiety for compound **1**, **2**, and **3**, respectively. Consequently, this part of the molecules seems to have the most pronounced hydrogen bond acceptor character. The results of the calculations clearly suggest that the excitation significantly decreases the electron density on these atoms and electron displacement occurs towards the triazine ring. Fig. 5 indicates that the charge shift upon excitation is larger for **2** and **3** compared to **1**.

3.4. *Flash photolysis studies*

Laser flash photolysis of **1** and **2** in toluene gives a short-lived species with absorption built up within the duration of the laser pulse. The transient decays on the microsecond time scale with lifetime 200 and 60 μs for **1** and **2**, respectively. The absorption spectra, recorded after the complete decay of the fluorescence in toluene, are presented in Fig. 6. These spectra are assigned to triplet–triplet absorption based on the following arguments: (i) in the presence of oxygen the transients were quenched; (ii) addition of

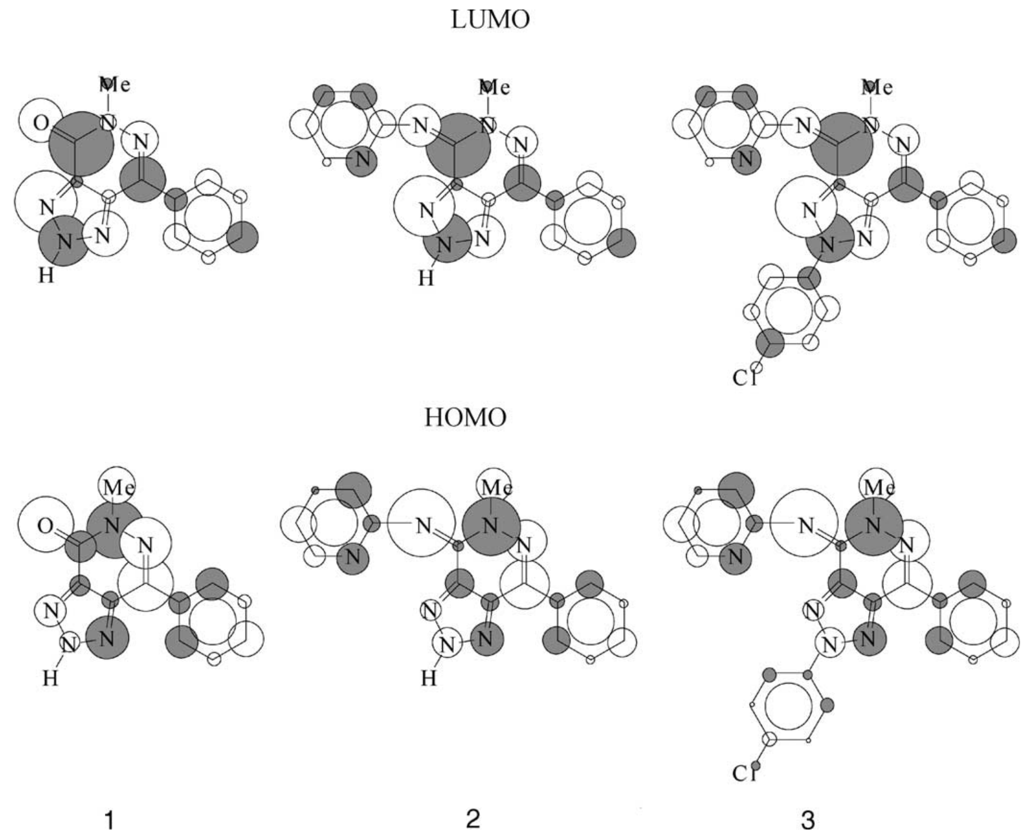

Fig. 5. Result of molecule orbital calculations with Hückel method.

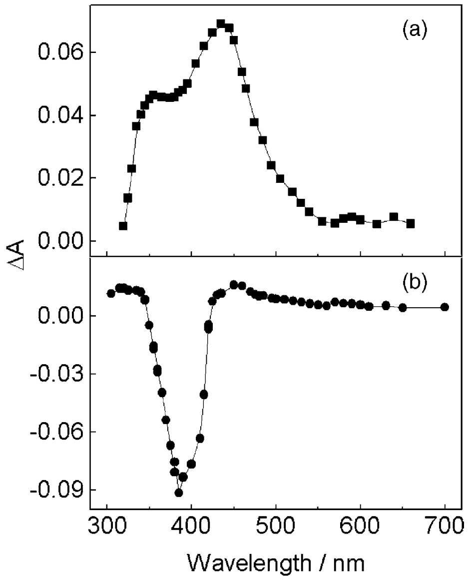

Fig. 6. Triplet–triplet absorption spectrum of: (a) **1** and (b) **2** in toluene.

perylene shortened the decay time of the transient and concomitant formation of triplet perylene was observed (vide infra). For compound **2**, significant bleaching can be observed in the 360–410 nm spectral range, which corresponds to the strong band in the ground state absorption spectrum. In the case of **1**, the ground state absorbs at higher energy, thus, bleaching in the triplet–triplet absorption spectrum appears below 320 nm. No significant difference is found in the triplet lifetime in ethanol and non-hydroxylic solvents and no long-lived absorption, which could be attributed to ketyl radical, appears after the complete decay of the triplet. These facts indicate that no hydrogen abstraction takes place with alcohols and the lowest triplet state of both **1** and **2** has $\pi\pi^*$ character.

Addition of increasing amount (5×10^{-5} to 2×10^{-4} M) of perylene gradually shortened the triplet lifetime of the studied compounds and the growing in of the well-established absorption of triplet perylene at 490 nm was observed [9]. The rate of the energy transfer was diffusion controlled ($k_q > 3\times10^9\ \mathrm{M^{-1}\,s^{-1}}$) indicating that the triplet energy for **1** and **2** is higher than that of perylene (148 kJ mol^{-1}) [9]. The efficient triplet sensitization of perylene was exploited to determine the triplet yield (Φ_{ISC}) from the triplet perylene absorbance at 490 nm in the solution of **1** and **2** (A) relative to that in the reference solution (A_{ref}) which had matched optical density at the laser wavelength (308 nm).

$$\Phi_{\mathrm{ISC}} = (\Phi_{\mathrm{ISC}})_{\mathrm{ref}}\left(\frac{A}{A_{\mathrm{ref}}}\right) \tag{3}$$

Fluorenone in toluene was chosen as a reference as it has a well-established triplet yield ($(\Phi_{\mathrm{ISC}})_{\mathrm{ref}} = 0.93$) [10]. Because of the low molar absorption coefficient of perylene in the ground state at 308 nm and the very low triplet yield ($\Phi_{\mathrm{ISC}} = 0.014$) [9], almost negligible amount of triplet perylene formed via direct excitation. The very small transient absorption arising from the direct excitation of perylene was measured in the absence of sensitizer and it was subtracted from the signals obtained in solutions containing sensitizer. The 2×10^{-4} M perylene concentration ensured that more than 98% of the triplet energy donors transferred their energy to perylene. The solvent dependence of triplet yields determined by this technique showed good agreement with the results of the other method where the initial triplet–triplet absorbance of the investigated compound was compared in various solvents.

The triplet yield of **3** was 0.02 in toluene and negligible triplet–triplet absorption was observed in more polar solvents. As this compound barely emits fluorescence, we can conclude that internal conversion is so rapid that no other energy dissipation pathways of the singlet excited state is able to compete with it.

3.5. Yield and rate constant of deactivation processes

Table 1 summarises the photophysical properties of **1**, **2** and their hydrogen-bonded complex measured in the presence of 0.03 M HFIPA. As no photochemical reaction was observed, the internal conversion yield (Φ_{IC}) was derived from the measured fluorescence (Φ_{F}) and triplet yields (Φ_{ISC}):

$$\Phi_{\mathrm{IC}} = 1 - \Phi_{\mathrm{F}} - \Phi_{\mathrm{ISC}} \tag{4}$$

The solvents were chosen to include apolar, polar aprotic and polar hydrogen bonding media. It is evident from the data in Table 1 that internal conversion is the dominant process from the singlet excited state in all cases. Triplet yields and fluorescence lifetimes are considerably larger for **1** compared to **2**. The change of the molecular structure and solvent scarcely affects the fluorescence yield.

To get a deeper insight into the factors controlling the competition among the deactivation pathways of the singlet excited molecules, the rate constants for fluorescence emission (k_{F}), intersystem crossing (k_{ISC}) and internal conversion (k_{IC}) were derived using the expressions given below:

$$k_{\mathrm{ISC}} = \frac{\Phi_{\mathrm{ISC}}}{\tau_{\mathrm{F}}} \tag{5}$$

$$k_{\mathrm{IC}} = \frac{1 - \Phi_{\mathrm{ISC}} - \Phi_{\mathrm{F}}}{\tau_{\mathrm{F}}} \tag{6}$$

$$k_{\mathrm{F}} = \frac{\Phi_{\mathrm{F}}}{\tau_{\mathrm{F}}} \tag{7}$$

The results are summarised in the last three columns of Table 1. It is clearly seen that k_{ISC} values for **1** and **2** are very similar and slightly diminish with increasing solvent polarity. The same tendency appears for the radiative rate constant of **1**; on the other hand, k_{F} enhancement is found in more polar media for **2**. The opposite solvent effect on k_{F}

can be rationalised in terms of the Strickler–Berg equation [11]:

$$k_{\mathrm{r}} = 2.88 \times 10^{-9} n^2 (\bar{\nu}^{-3})_{\mathrm{av}}^{-1} \int \varepsilon \, \mathrm{d} \ln \bar{\nu} \qquad (8)$$

where n is the refractive index of the solvent, $(\bar{\nu}^{-3})_{\mathrm{av}}^{-1}$ denotes an average over the fluorescence spectrum and the integral extends over the first absorption band. As the relationship predicts that k_{F} increases approximately as the cube of the emission energy, the solvent dependence of k_{F} is determined mainly by the displacement of the fluorescence maximum. Therefore, k_{F} becomes larger when the fluorescence band of **2** moves to higher energy, whereas the red-shift of the fluorescence spectrum of **1** with increasing solvent polarity leads to lower k_{F} values.

It is seen in Table 1 that the short fluorescence lifetime of **2** is due to the rapid internal conversion. The significantly higher k_{IC} of this compound is in accord with the prediction of the energy gap law which suggest an exponential dependence of the deactivation rate on the energy difference between the excited and the ground states. As the energy of the lowest singlet excited state of **2** is about 60 kJ mol^{-1} lower than that of **1**, the radiationless relaxation to the ground state is markedly accelerated for the former compound. Although, ring opening followed by reaction back to the original compound after crossing to the ground state potential surface could lead to efficient energy dissipation, no evidence has been found for this process. The fast internal conversion is probably the consequence of vibronic coupling between close-lying $n\pi^*$ and $\pi\pi^*$ singlet excited states, which is called as proximity effect [12]. E.C. Lim demonstrated that the proximity effect plays a key role in the photophysics of many nitrogen heterocyclic and aromatic carbonyl compounds [13].

The data in Table 1 demonstrate that hydrogen bonding has little impact on the energy and the relaxation kinetics of the singlet excited molecules. The increase of the fluorescence lifetime and yield on hydrogen bonding is attributed to the deceleration of the internal conversion in the complex. This effect is opposite to that found for anthraquinone [14] and fluorenone derivatives [15], where efficient energy dissipation occurs via the hydrogen bond. Systematic studies on the excited hydrogen-bonded complexes of 2-substituted fluorenones revealed that the electron-density around the carbonyl oxygen controls the radiationless deactivation [16] and correlation was found between the excited state dipole moment and the rate of the hydrogen bonding induced internal conversion. It was demonstrated that the interaction with alcohols in the excited state results in efficient internal conversion only if the hydrogen bonding strength in the excited state is significantly higher than in the ground state [16,17]. These previous results are corroborated by the lack of hydrogen bonding induced quenching for **1** and **2**. In these compounds, hydrogen bonding does not stabilise the excited state relative to the ground state because $E(\mathrm{S}_1)$ barely differs for the free and the complexed molecules (Table 1). Theoretical calculations showed that no dipole moment enhancement takes place upon light absorption thus, hydrogen bonding can not be stronger in the excited state and the photophysical properties of the free and the hydrogen-bonded molecules are fairly similar.

Acknowledgements

We very much appreciate the support of this work by the 1/047 NKFP Medichem Project and the Hungarian Scientific Research Fund (OTKA, Grant T034990).

References

[1] B.U.W. Maes, O. R‘kyek, J. Kosmrlj, G.L.F. Lemiére, E. Esmans, J. Rozenski, R.A. Dommisse, A. Haemers, Tetrahedron 57 (2001) 1323.

[2] K.C.V. Ramanaiah, E.D. Stevens, M.L. Trudell, J. Heterocycl. Chem. 37 (2000) 1597.

[3] (a) Y. Nagawa, K. Honda, H. Nakanishi, Heterocycles 51 (1999) 1093;
(b) M. Kurumi, K. Sasaki, H. Takata, T. Nakayama, Heterocycles 53 (2000) 2809.

[4] P. Kövér, Gy. Hajós, Zs. Riedl, L. Párkányi, G. Kollenz, Chem. Commun. (2000) 1785.

[5] (a) D.F. Eaton, Pure Appl. Chem. 60 (1988) 1107;
(b) W.H. Melhuish, J. Phys. Chem. 65 (1961) 229.

[6] A. Demeter, L. Biczók, T. Bérces, V. Wintgens, P. Valat, J. Kossanyi, J. Phys. Chem. 97 (1993) 3217.

[7] W.J. Middleton, R.V. Lindsey Jr., J. Am. Chem. Soc. 86 (1964) 4948.

[8] N. Mataga, T. Kubota, Molecular Interactions and Electronic Spectra, Marcel Dekker, New York, 1970, p. 348.

[9] S.L. Murov, G.L. Carmichael, I. Hug, Handbook of Photochemistry, 2nd ed., Marcel Dekker, New York, 1993.

[10] (a) R.A. Caldwell, R.P. Gajewski, J. Am. Chem. Soc. 93 (1971) 533;
(b) A.A. Lamola, G.S. Hammond, J. Chem. Phys. 43 (1965) 2129;
(c) L.J. Andrews, A. Deroulede, H. Linschitz, J. Phys. Chem. 82 (1978) 2304.

[11] S.J. Strickler, R.A. Berg, J. Chem. Phys. 37 (1962) 814.

[12] E.C. Lim, Excited States, vol. 3, Academic Press, New York, 1977, p. 305.

[13] E.C. Lim, J. Phys. Chem. 90 (1986) 6770.

[14] (a) H. Inoue, M. Hida, N. Nakashima, K. Yoshihara, J. Phys. Chem. 86 (1982) 3184;
(b) S.R. Flom, P.F. Barbara, J. Phys. Chem. 89 (1985) 4489;
(c) J. Ritter, H.U. Borst, T. Lindner, M. Hauser, S. Brosig, K. Bredereck, U.E. Steiner, D. Kühn, J. Kelemen, H.E.A. Kramer, J. Photochem. Photobiol. A 41 (1988) 227;
(d) H.U. Borst, J. Kelemen, J. Fabian, M. Nepras, H.E.A. Kramer, J. Photochem. Photobiol. A 69 (1992) 97.

[15] (a) L. Biczók, T. Bérces, H. Linschitz, J. Am. Chem. Soc. 119 (1997) 11071;
(b) T. Yatsuhashi, Y. Nakajima, T. Shimada, H. Tachibana, H. Inoue, J. Phys. Chem. A 102 (1998) 8657;
(c) T. Yatsuhashi, H. Inoue, J. Phys. Chem. A 101 (1997) 8166;
(d) M. Sugita, T. Shimada, H. Tachibana, H. Inoue, Phys. Chem. Chem. Phys. 3 (2001) 2012;
(e) T. Yatsuhashi, Y. Nakajima, T. Shimada, H. Inoue, J. Phys. Chem. A 102 (1998) 3018.

[16] L. Biczók, T. Bérces, H. Inoue, J. Phys. Chem. A 103 (1999) 3837.

[17] L. Biczók, T. Bérces, T. Yatsuhashi, H. Tachibana, H. Inoue, Phys. Chem. Chem. Phys. 3 (2001) 980.

[18] C. Reichardt, Solvent Effects in Organic Chemistry, Verlag Chemie, Weinheim, 1979.